

Hyperpolarization-activated Chloride Currents in *Xenopus* Oocytes

GOPAL C. KOWDLEY, STEPHEN J. ACKERMAN, J. EDWARD JOHN, III,
LARRY R. JONES,* and J. RANDALL MOORMAN

From the Departments of Internal Medicine (Cardiovascular Division), and Molecular Physiology and Biological Physics, University of Virginia Health Sciences Center, Charlottesville, Virginia 22908; and *Departments of Internal Medicine and Biochemistry, Krannert Institute of Cardiology, Indiana University School of Medicine, Indianapolis, Indiana 46202

ABSTRACT During hyperpolarizing pulses, defolliculated *Xenopus* oocytes have time- and voltage-dependent inward chloride currents. The currents vary greatly in amplitude from batch to batch; activate slowly and, in general, do not decay; have a selectivity sequence of $I^- > NO_3^- > Br^- > Cl^- > \text{propionate} > \text{acetate}$; are insensitive to Ca^{2+} and pH; are blocked by Ba^{2+} and some chloride channel blockers; and have a gating valence of ~ 1.3 charges. In contrast to hyperpolarization-activated chloride currents induced after expression of phospholemman (Palmer, C. J., B. T. Scott, and L. R. Jones. 1991. *Journal of Biological Chemistry*. 266:11126; Moorman, J. R., C. J. Palmer, J. E. John, J. E. Durieux, and L. R. Jones. 1992. 267:14551), these endogenous currents are smaller; have a different pharmacologic profile; have a lower threshold for activation and lower voltage-sensitivity of activation; have different activation kinetics; and are insensitive to pH. Nonetheless, the endogenous and expressed current share striking similarities. Recordings of macroscopic oocyte currents may be inadequate to determine whether phospholemman is itself an ion channel and not a channel-modulating molecule.

INTRODUCTION

Xenopus oocytes have at least two kinds of hyperpolarization-activated Cl^- currents. Parker and Miledi (1988) reported a Ca^{2+} -insensitive, noninactivating I_{Cl} , and Miledi (1982) and Peres and Bernardini (1983) described another I_{Cl} which is Ca^{2+} -sensitive and inactivates over several seconds. We have further characterized the Ca^{2+} -insensitive, noninactivating hyperpolarization-activated I_{Cl} , which we call $I_{Cl(\text{endo})}$. A major goal was to compare and contrast $I_{Cl(\text{endo})}$ with another hyperpolarization-activated I_{Cl} which is induced after oocyte expression of phospholemman (PLM), a 72 amino acid membrane protein which is a major substrate for protein kinases A and C (Palmer, Scott, and Jones, 1991). We call this expressed current $I_{Cl(\text{PLM})}$ (Moorman, Palmer, John, Durieux, and Jones, 1992). $I_{Cl(\text{endo})}$ has several characteristics in common with $I_{Cl(\text{PLM})}$, and allows the possibility that PLM may modify $I_{Cl(\text{endo})}$.

Address correspondence to J. Randall Moorman, Box 6012, MR4 Building, University of Virginia Health Sciences Center, Charlottesville, VA 22908.

MATERIALS AND METHODS

Oocyte Preparation

Our methods for oocyte isolation, RNA preparation and injection, and microelectrode voltage clamping have been described (Durieux, Salafranca, Lynch, and Moorman, 1992; Moorman *et al.*, 1992). In this study, oocytes were evaluated 1 to 10 d after isolation and were defolliculated manually the day of or one day before electrophysiologic study.

Electrophysiological Analysis

Membrane currents were measured with a two-microelectrode voltage clamp (OC-725, Warner Instruments, New Haven, CT) and pCLAMP (Axon Instruments, Foster City, CA). Microelectrodes were beveled to resistances of 1–3 M Ω and contained (in mM): KCl 3000, EGTA 10, HEPES 10 (pH 7.3). Hyperpolarizing and depolarizing pulses were administered from a holding potential of –10 mV at 0.1–0.15 Hz. Currents were filtered at 40 Hz and sampled at 0.5 to 1 kHz. The external solution was perfused at 3–4 ml/min and contained (mM): NaCl 150, KCl 5, CaCl₂ 2, MgCl₂ 1, dextrose 10, and HEPES 10 (pH 7.4, NaOH). Data are represented as mean \pm standard deviation unless noted otherwise. Current waveforms were fit to a sum of two exponentials function of the form:

$$I(t) = I_0 + A_1 \exp(-t/\tau_1) + A_2 \exp(-t/\tau_2).$$

For measurement of reversal potentials, the chamber was initially perfused with a solution that contained (mM): NaCl 20, KCl 5, CaCl₂ 2, MgCl₂ 1, dextrose 10, MES 180, and HEPES 10 (pH 7.4). The perfusate was changed by a series of solutions in which MES was replaced by Cl[–]. The Cl[–] concentrations were (mM) 31, 47, 75, 123, and 211. Currents were activated by 1–3 s voltage steps to –160 to –220 mV, then the voltage was changed to values between –60 and 30 mV in steps of 2.5 to 10 mV. The decay phase of the tail currents was fit to an exponential function, and the extrapolated initial amplitudes were plotted as a function of tail potential. The interpolated x-intercept of this plot was taken as the reversal potential.

For measurement of the steepness of the voltage dependence of gating of the current, we measured the peak amplitude of tail currents after hyperpolarizing steps. After a 2-s hyperpolarizing step to potentials between –30 and –160 mV in decrements of 10 mV, the voltage was stepped to 10 or 40 mV. These potentials were selected because they do not significantly activate the endogenous Ca²⁺-activated Cl[–] current $I_{Cl(Ca)}$ (Miledi, 1982; Barish, 1983). Tail current amplitudes were normalized for each oocyte by dividing by the amplitude of the largest tail current. The derived values are equivalent to the probability of opening, or P_o . The log of P_o was plotted as a function of hyperpolarizing conditioning pulse potential, and a straight line was plotted through the values of P_o between 0.01 and 0.1. The gating valence z , which reflects the minimum number of charges traversing the full thickness of the membrane during channel opening (Hille, 1992), is related to the slope of the line, $\log P_o/V$:

$$z = 2.303 \frac{RT \log P_o}{F V}$$

where R , T , and F have their usual meanings.

For measurement of permeability ratios P_X/P_{Cl} , we measured reversal potentials in solutions with concentrations (mM): NaX 150, HEPES 20, dextrose 10, Ca(OH)₂ 1 (pH 6.5 to 7.0) where X corresponds to Cl[–], Br[–], NO₃[–], I[–], acetate, and propionate. Oocytes were first tested in the Cl[–] solution. The second solution was perfused at a rate of 3–4 ml/min until the bath volume of 3 ml had been exchanged at least 8 to 10 times. The reversal potentials were determined as described above. Each oocyte was tested once in Cl[–] and once in one other anion solution, and

was then discarded. The permeability ratios were calculated as (Hille, 1992):

$$\frac{P_X}{P_{Cl^-}} = \exp \frac{\Delta E_{rev} z F}{RT}$$

where $\Delta E_{rev} = (E_{rev,X} - E_{rev,Cl})$. We assumed that the internal concentration of ions was constant during the period of measurement.

The Cl^- channel blocking agents niflumic acid, bumetanide, 4,4'-diisothiocyanostilbene-2,2'-disulfonic acid (DIDS), 4-acetamido-4-isothiocyanostilbene-2,2'-disulfonic acid (SITS), and anthracene-9-carboxylic acid (9-AC) (all from Sigma Chemical Co., St. Louis, MO) were prepared at concentrations of 1 or 2 mM solutions in the standard external solution. After measurement of the current-voltage relationship in the external solution alone, we perfused the recording chamber with 8 to 10 bath volumes of the external solution with a blocking agent and repeated the measurement. Each oocyte was tested once with one blocking agent and then discarded. We measured the difference in current amplitude from the beginning to the end of 2-s pulses to a test potential of -150 or -190 mV, and we tabulated the ratio of this amplitude in the presence of blocker to the same measurement in the absence of blocker.

RESULTS

Endogenous Hyperpolarization-activated Currents Showed a Spectrum of Current Decay Kinetics

Fig. 1 shows hyperpolarization-activated currents elicited from defolliculated *Xenopus* oocytes. Though all activated relatively quickly, decay kinetics differed. The currents shown in *A* reached a peak and decayed, those in *C* continued to activate throughout the 2-s pulse, and those in *B* showed intermediate kinetics. Most of the currents we observed had kinetics similar to *C*. As an index of current kinetics, we measured the difference in current amplitude from 400 ms (or the peak, if there was one) to the end of the 2-s test pulse. *D* is a frequency histogram of the amplitude of these developed currents. Values less than 0 indicate noninactivating currents such as in *C*, and predominate the histogram.

Activation kinetics could be described as a sum of two exponentials. In 11 oocytes from four batches with large, noninactivating currents at a test potential of -140 mV, the time constants (and relative weights) were 200 ± 96 ms (0.29 ± 0.15) and $13,230 \pm 8,055$ ms (0.71 ± 0.15).

Parker and Miledi (1988) found that the magnitude of $I_{Cl(endo)}$ fell as the number of days after oocyte isolation increased. This phenomenon was not prominent in our experience with $I_{Cl(endo)}$. Generally, the amplitude of $I_{Cl(endo)}$ did not vary predictably. For example, from a single batch of oocytes ($n = 15$) studied on days 1, 3, 4, 5, and 7 after isolation, the mean currents at -150 mV were (μA): 8.7, 3.9, 8.3, 6.3, and 4.8 respectively.

Current Amplitudes Varied Among Batches of Oocytes

An important feature of $I_{Cl(endo)}$ is its variability among batches of oocytes. Fig. 2*A* is a boxplot of current amplitudes as a function of batch number. The 32 batches, from at least 15 frogs, were studied from June, 1992, to February, 1993. For this analysis, we subtracted the instantaneous current and measured the current developed during a 2-s pulse to a test potential of -150 mV. Variability of the current amplitudes is

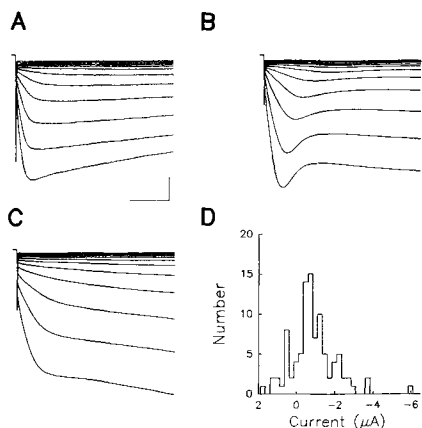


FIGURE 1. Kinetics of $I_{Cl(endo)}$. Currents were elicited during steps from a holding potential of -10 mV to test potentials of -30 to -160 mV in 10 mV decrements. There is no correction for leak or capacitance currents. Bar is 0.5 s and (A) 1 μ A, or (B, C) 2 μ A. The times to half-maximal activation at a test potential of -140 mV are (A) 64 ms, (B) 126 ms, and (C) 326 ms.

D is a histogram of current amplitudes from 98 oocytes with the largest currents from 22 batches. Current amplitude was measured as the difference

of $I_{400\text{ msec}}$ and $I_{2\text{ sec}}$ for currents without peaks (e.g., Fig. 1 C), or the difference between I_{peak} and $I_{2\text{ sec}}$. A negative value means that current increased throughout the trace; a positive number means that current decayed during the trace.

seen between batches and within batches. Generally, most batches of oocytes showed small currents at this test potential. Oocytes from 17 batches never had currents > 3 μ A, whereas others ranged up to 12.4 μ A. In batches of oocytes with large $I_{Cl(endo)}$, nearly every oocyte had currents. In batches with small or no $I_{Cl(endo)}$ at a test potential of -150 mV, currents could be elicited by hyperpolarization to -180 to -200 mV (e.g., Fig. 5 A). We could discern no phenotypic marker of frogs or oocytes with large $I_{Cl(endo)}$. Oocytes were Dumont stage V–VI and did not have germinal vesicle breakdown.

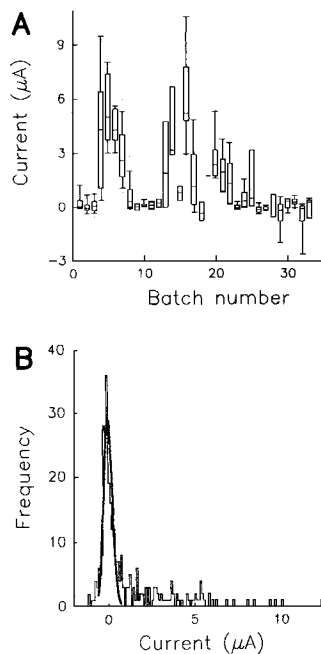


FIGURE 2. Variability of $I_{Cl(endo)}$ amplitude and kinetics. A is a boxplot of the currents at the end of a 2-s hyperpolarization pulse minus instantaneous current, from -10 mV to a test potential of -150 mV. The data are from 32 batches of oocytes with $n = 2$ to 32 oocytes. The line in the middle is the median; the box encompasses the 25th through 75th percentiles; the hatches encompass the 10th through the 90th. B is a frequency histogram of the current amplitudes. The smooth line is of the form:

$$F(I) = 1.8 \times 10^4 (0.26 \mu\text{A} \sqrt{2\pi})^{-1} \times \exp - \frac{(I + 0.01 \mu\text{A})^2}{2(0.26 \mu\text{A})^2}$$

and encompasses ~ 190 of the 299 current amplitudes.

Fig. 2 *B* is a frequency histogram of the same data as *A*. The median current amplitude of 299 oocytes was 0.24 μA (mean 1.1 μA , standard deviation 2.1 μA). Current amplitudes of about two-thirds of the oocytes belonged to a Gaussian distribution with a mean near 0 μA .

The Current Was Anion-selective

We measured the reversal potential for multiple values of $[\text{Cl}^-]_o$ (Fig. 3 *A*). As expected for Cl^- currents, the reversal potential became more negative as $[\text{Cl}^-]_o$ increased. The straight line is the expected relationship for channels permeable to

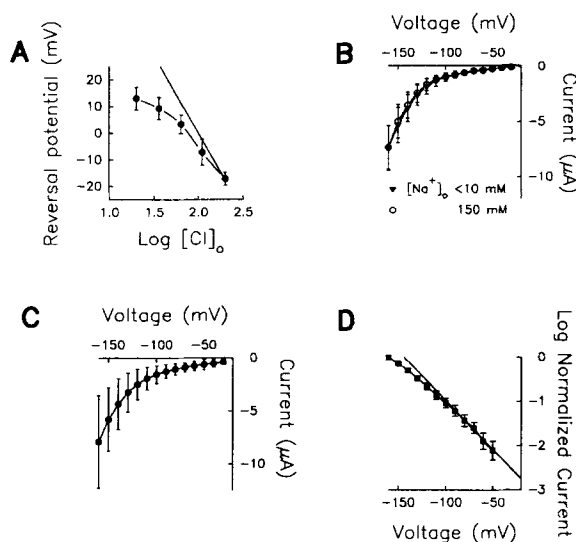


FIGURE 3. $I_{\text{Cl}(\text{endo})}$ is a voltage-dependent anion current. Panel A is a plot of reversal potential, measured from tail currents, as a function of $[\text{Cl}^-]_o$. Data points are the mean of six determinations in oocytes from a single frog; bars are standard deviation. The straight line is of the form:

$$E_{\text{rev}} = \frac{RT}{zF} \ln \frac{[\text{Cl}^-]_o}{100 \text{ mM}}$$

B is a plot of current amplitude at the end of a 2-s hyperpolarization pulse as a function of test potential, from a holding potential of -10 mV . Data points are the average of three

oocytes, and bars represent standard error. The oocytes were first bathed in a solution containing 150 mM NaCl which was changed to a solution in which *N*-methyl-D-glucamine-Cl replaced NaCl.

C shows the current-voltage relationship for 44 oocytes with large currents. Leak-uncorrected current amplitudes from oocytes were averaged; bars are standard deviation.

D shows the voltage sensitivity of activation gating. Tail currents were measured at potentials of $+10$ or $+40 \text{ mV}$ following hyperpolarization to potentials indicated along the x-axis; bars are standard error. The currents were normalized relative to the largest tail current for each oocyte. The straight line was fit to the points from 1 to 10% of the maximum tail current.

Cl^- alone. The deviation of the data at low $[\text{Cl}^-]_o$ concentrations suggests that other ions are permeant as well. Other Cl^- channels are imperfectly selective (Hille, 1992). Na^+ has been reported to be necessary for Cl^- conduction in other Cl^- channels (Bahinski *et al.*, 1989; Matsuoka *et al.*, 1990). We replaced Na^+ with *N*-methyl-D-glucamine and saw no change in current amplitude (Fig. 3 *B*).

The Selectivity Followed the Lyotropic Sequence

In nine oocytes, the reversal potential shifted an average of -22 mV when NaI was substituted for NaCl in the bathing solution. This indicates that I^- was more

permeant than Cl^- , and $P_{\text{I}}/P_{\text{Cl}} = 2.45$. Overall, the current had a selectivity profile of $\text{I}^- > \text{NO}_3^- > \text{Br}^- > \text{Cl}^- > \text{propionate} > \text{acetate}$ with ratios of: 2.5: 2.0: 1.4: 1.0: 0.35: 0.17, respectively. In similar experiments, we found the selectivity profile of $\text{I}_{\text{Cl(PLM)}}$ also to be $\text{I}^- > \text{NO}_3^- > \text{Br}^- > \text{Cl}^-$, with ratios of 1.9: 1.7: 1.6: 1.0. Four to nine oocytes were tested for each anion. This sequence is similar to that of other Cl^- channels (Franciolini and Nonner, 1987), and follows the lyotropic or Hofmeister sequence (Hille, 1992).

The Gating Valence Was Low

The current-voltage relationship (Fig. 3 C) shows that the current was activated by hyperpolarizing voltage steps, but the threshold for activation is not clear. At potentials in the range of -30 mV, near E_{Cl} , the combination of low probability of channel opening and small unitary currents may have made active currents too small

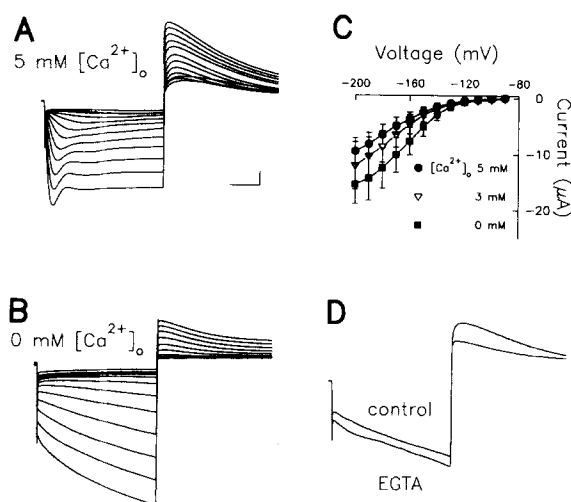


FIGURE 4. $\text{I}_{\text{Cl(endo)}}$ is Ca^{2+} -insensitive. *A* and *B* show currents elicited by hyperpolarizing steps from -10 mV to test potentials between -90 and -200 in an oocyte in two concentrations of $[\text{Ca}^{2+}]_o$. Averaged current-voltage relationships are shown in *C* for six oocytes in solutions of varying $[\text{Ca}^{2+}]_o$; bars are standard error. *D* shows the average of currents elicited at test potential of -150 mV in two oocytes before and after intracellular injection of 50 nl of a 100-mM EGTA solution. The tail potential is 40 mV, and the bar is 0.5 s and 1 μA for all currents in the figure.

to detect. To clarify the voltage dependence of activation, we measured tail currents at positive potentials following 2-s hyperpolarizing steps. Fig. 3 *D* shows a semilogarithmic plot of normalized tail current amplitudes as a function of the voltage of the hyperpolarizing step. The straight line was fit by linear regression, and its slope yields an estimated gating valence of 1.3 charges. From this plot, we estimate that between 0.1% and 1% channels were open during steps to -30 or -40 mV.

The Current Did Not Require Ca^{2+} for Activity

Fig. 4, *A* and *B*, show currents from the same oocyte bathed in 5 mM Ca^{2+} and in nominally 0 mM Ca^{2+} . In these experiments, $[\text{Mg}^{2+}]_o$ was adjusted so that the total divalent concentration was 5 mM. As shown previously (Peres and Bernardini, 1983; Taglietti, Tanzi, Romero, and Simoncini, 1984; Parker, Gunderson, and Miledi, 1985), there was a fast-activating, fast-inactivating component of the current that was

enhanced by $[Ca^{2+}]_o$. The amplitude of the current at the end of the trace, however, did not decrease as $[Ca^{2+}]_o$ was varied. Fig. 4 C is an current-voltage relationship showing the effect of $[Ca^{2+}]_o$ on the amplitude of $I_{Cl(endo)}$. There was no significant change when $[Ca^{2+}]_o$ was varied from 0 to 5 mM, suggesting that $I_{Cl(endo)}$ did not require $[Ca^{2+}]_o$ for its activity. In fact, $I_{Cl(endo)}$ increased in magnitude as $[Ca^{2+}]_o$ fell, though the change was not large or statistically significant. D shows that there is no significant change in the current after EGTA injection to an estimated oocyte concentration of 5 mM ($n = 4$). Thus, neither extracellular nor intracellular Ca^{2+} appear mandatory for activation of $I_{Cl(endo)}$.

The Current Was Blocked by Ba^{2+} But Not by Protons

Fig. 5 A shows that $I_{Cl(endo)}$ was blocked by $[Ba^{2+}]_o$, with an IC_{50} of 0.18 mM ($n = 8$). The current-voltage relationship (*inset*) did not shift along the voltage axis, suggesting that a shift in voltage-dependent gating is not the mechanism of block. The block was not readily reversible, and higher concentrations of Ba^{2+} were added sequentially. In these oocytes, $I_{Cl(endo)}$ was small, and large hyperpolarizations were required to elicit measurable currents.

Because low pH_o activates a hyperpolarization-activated Cl^- conductance in *Xenopus* skeletal muscle (Vaughan, 1991) and increases the amplitude of $I_{Cl(PLM)}$ (Moorman *et al.*, 1992), we tested the effect of pH_o on the amplitude of $I_{Cl(endo)}$. Fig. 5 B shows current-voltage relationships over a range of pH_o . They are very similar, suggesting that $I_{Cl(endo)}$ is insensitive to variation in pH_o in the range of 6.5 to 8.0.

The Current Was Blocked by Cl^- Channel Blockers

Table I summarizes experiments in which we measured the amplitude of $I_{Cl(endo)}$ at a test potential of -150 or -190 mV in the absence and presence of Cl^- channel blocking agents. The extent of block was variable, and no agent was a potent blocker. Surprisingly, the two disulfonic acid derivatives SITS and DIDS gave different results. DIDS had no consistent blocking effect—the mean $I_{Cl(endo)}$ amplitude increased slightly—while SITS blocked more than any other agent we tested (Fig. 5, C and D).

Table I also shows the effects of these agents on $I_{Cl(PLM)}$. There are some important differences. Most notably, DIDS blocked $I_{Cl(PLM)}$ by $\sim 80\%$ and was equivalent to SITS.

DISCUSSION

We studied hyperpolarization-activated Cl^- currents endogenous to defolliculated *Xenopus* oocytes. These currents were first reported by Parker and Miledi (1988), who described their activation by hyperpolarization, dependence of reversal potential on $[Cl^-]_o$, and independence of $[Ca^{2+}]_o$. Our most important new findings are (a) current amplitudes are variable from one batch of oocytes to the next, (b) the current does not depend on extracellular or intracellular Ca^{2+} , or on extracellular Na^+ , (c) permeability ratios follow the lyotropic or Hofmeister sequence, (d) the equivalent gating valence is much lower than for K^+ or Na^+ channels, (e) the current is active at very modest hyperpolarization, (f) the current is blocked by $[Ba^{2+}]_o$ and some Cl^- channel blockers, especially SITS, and (g) the current is insensitive to variations in external pH in the range of 6.5 to 8.0.

Comparison with Other Chloride Currents

$I_{Cl(\text{endo})}$ is easily distinguished from another kind of inactivating hyperpolarization-activated Cl^- current in amphibian oocytes which requires both extracellular and intracellular Ca^{2+} (Peres and Bernardini, 1983; Taglietti *et al.*, 1984; Parker *et al.*, 1985). This current, which is sometimes present endogenously and is accentuated

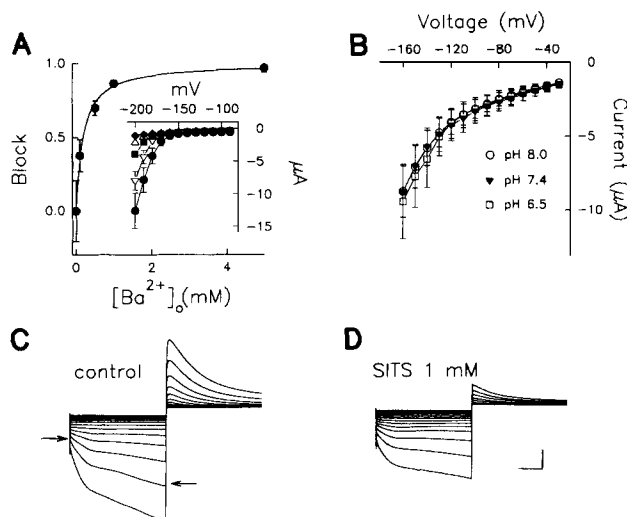


FIGURE 5. Block and pH dependence of $I_{Cl(\text{endo})}$. *A* shows the concentration-dependence of block of currents in four oocytes for four concentrations of Ba^{2+} at a test potential of -160 mV; bars are standard error. The line is a single site binding model of the form:

$$\text{block} = B_{\text{max}} \frac{[\text{Ba}^{2+}]_o}{[\text{Ba}^{2+}]_o + 0.18 \text{ mM}}$$

where B_{max} is the maximum block, and 0.18 is the IC_{50} . The inset shows the current-voltage relationships for the same four oocytes; bars are standard error. $[\text{Ba}^{2+}]$ was (mM) 0 (●), 0.1 (▽), 0.5 (■), 1 (△), and 5 (◆). Currents were measured at the end of a 2-s hyperpolarization pulse from a holding potential of -10 mV to test potentials of -90 to -200 mV in decrements of 10 mV.

B shows the current-voltage relationship for seven oocytes where pH_o was varied; bars are standard error. Currents were measured at the end of a 2-s hyperpolarization to potentials of -30 to -160 mV from a resting potential of -10 mV.

C and *D* are currents in the same oocyte before and after perfusion with SITS 1 mM. Holding potential was -10 mV; test potentials were -30 to -160 mV. At a test potential of -150 mV, the current amplitude (measured as the difference of the two current levels marked by arrows) fell from 4.40 to 2.23 μA , signifying 50.6% block. Bar is 0.5 s and 2 μA .

after injection of brain mRNA and subsequent application of peptide hormones such as serotonin (Parker *et al.*, 1985), was rarely observed in the course of our studies (Fig. 4 *A*).

Hyperpolarization-activated Cl^- currents with slow kinetics have also been characterized in *Aplysia* neurons (Chesnoy-Marchais, 1982, 1983) and, at low pH, in

amphibian skeletal muscle (Warner, 1972; Loo, McLaron, and Vaughn, 1981). Large conductance Cl^- channels have been reported from multiple tissues, including heart (Coulombe, Duclotier, Coraboeuf, and Touzet, 1987; Coulombe and Coraboeuf, 1992), skeletal muscle (Blatz and Magleby, 1983; Schwarze and Kobl, 1984; Woll, Leibowitz, Neumcke, and Hille, 1987) and smooth muscle (Saigusa and Kokubun, 1988; Soejima and Kokubun, 1988; Kokubun, Saigusa, and Tamura, 1991).

Recently, it has been suggested that the cystic fibrosis transmembrane regulator protein (CFTR) is a Cl^- channel which is regulated by intracellular cAMP (Rich, Gregory, Anderson, Manavalin, Smith, and Welsh, 1991; Bear, Duguay, Naismith, Kartner, Hanratian, and Riordan, 1991; Anderson, Gregory, Thompson, Souza, Paul, Mulligan, Smith, and Welsh, 1991). In addition, a cardiac Cl^- channel that is activated by β -adrenergic agonists (Harvey and Hume, 1989; Bahinski, Nairn, Greengard, and Gadsby, 1989; Ehara and Ishihara, 1990; Matsuoka, Ehara, and Noma, 1990) may well be the product of a cardiac CFTR gene (Levesque, Hart, Hume, Kenyon, and Horowitz, 1992). This and other cardiac Cl^- currents and channels have been recently reviewed (Ackerman and Clapham, 1993). The identity

TABLE I
Block of $I_{\text{Cl}(\text{endo})}$ and $I_{\text{Cl}(\text{PLM})}$ by Cl^- Channel Blockers

AGENT	$I_{\text{Cl}(\text{endo})}$ % BLOCK	oocytes (frogs)	$I_{\text{Cl}(\text{PLM})}$ % BLOCK	oocytes (frogs)
	<i>SD</i>		<i>SD</i>	
DIDS* 1 mM	-13.7 (31.9)	11 (3)	70.1 (19.1)	6 (3)
Niflumic acid 1 mM	2.7 (36.0)	13 (3)	40.8 (25.6)	7 (3)
9-AC 1 mM [†]	14.1 (19.6)	12 (3)	27.2 (16.0)	5 (3)
Bumetanide 1 mM	15.9 (40.4)	11 (3)	29.7 (20.1)	7 (2)
SITS 1 mM [‡]	37.7 (26.8)	13 (3)	78.9 (5.5)	5 (2)

*DIDS, 4,4'-diisothiocyanostilbene-2,2'-disulfonic acid; [†]9-AC, anthracene-9-carboxylic acid; [‡]SITS, 4-acetamido-4-isothiocyanostilbene-2,2'-disulfonic acid.

of CFTR as an ion channel, though, has recently been challenged (Gabriel, Clarke, Boucher, and Stutts, 1993). These currents differ significantly from $I_{\text{Cl}(\text{endo})}$ and $I_{\text{Cl}(\text{PLM})}$ in at least two ways: there is little voltage-dependence of gating—the CFTR and cardiac currents, once stimulated, persist at all voltages—and extracellular Na^+ is required, at least for the cardiac Cl^- current (Bahinski *et al.*, 1989; Matsuoka *et al.*, 1990).

Cl^- channel cDNA has now been cloned from a number of sources by Jentsch and co-workers (Jentsch, Steinmeyer, and Schwarz, 1990; Steinmeyer, Ortland, and Jentsch, 1991; Thiemann, Gründer, Pusch, and Jentsch, 1992). One, which they named ClC-2 , induces hyperpolarization-activated Cl^- currents in mRNA-injected *Xenopus* oocytes (Thiemann *et al.*, 1992). This current has some kinetic similarities to $I_{\text{Cl}(\text{endo})}$; however, it has a different selectivity profile. It has been recently shown to be activated by changes in osmolarity, and experiments with oocyte-expressed ClC-2 mutants have led to identification of domains within the channel protein responsible for this modulation (Gründer, Thiemann, Pusch, and Jentsch, 1992).

Is Phospholemman an Ion Channel, or Does it Modulate $I_{Cl(endo)}$?

We have reported that expression of phospholemman (PLM), a 72 amino acid peptide with a single transmembrane region (Palmer *et al.*, 1991), induces hyperpolarization-activated Cl^- currents in *Xenopus* oocytes (Moorman *et al.*, 1992). Because mutations in the hydrophobic region altered activation kinetics, we speculated that PLM was an ion channel molecule. During the course of those experiments, we did

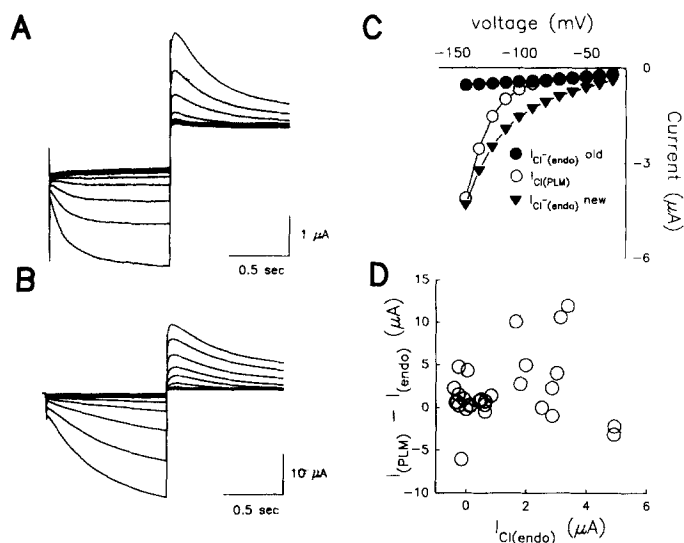


FIGURE 6. Comparison of $I_{Cl(endo)}$ and $I_{Cl(PLM)}$. *A* and *B* show families of currents elicited by hyperpolarization in oocytes from the same frog, one of which had not been injected with RNA (*A*), and the other injected with mRNA for PLM (*B*). $I_{Cl(PLM)}$ was much larger—the calibration bar is $1 \mu A$ for $I_{Cl(endo)}$ and $10 \mu A$ for $I_{Cl(PLM)}$ —and had much slower onset. Currents were elicited by 2-s voltage steps of -30 to -160 mV in decrements of 10 mV followed by 2-s steps to 40 mV.

C shows current-voltage relationships for uninjected oocytes with large $I_{Cl(endo)}$ from this report ($I_{Cl(endo)}$ new, $n = 44$), oocytes expressing PLM in batches of oocytes with little or no $I_{Cl(endo)}$ ($I_{Cl(PLM)}$), and uninjected oocytes with little or no $I_{Cl(endo)}$ ($I_{Cl(endo)}$ old). The latter two data sets are from reference (Moorman *et al.*, 1992).

D depicts the correlation between $I_{Cl(endo)}$ and $I_{Cl(PLM)}$ amplitudes. Each data point represents a batch of oocytes for which multiple measurements of $I_{Cl(endo)}$ and $I_{Cl(PLM)}$ were made. The ordinate is mean $I_{Cl(PLM)}$ minus mean $I_{Cl(endo)}$, or the increase in I_{Cl} after PLM expression. The abscissa is the mean $I_{Cl(endo)}$.

not observe the endogenous hyperpolarization-activated Cl^- current described here. Fig. 6 *C* shows current-voltage relationships for three kinds of oocytes. The circles are data from (Moorman *et al.*, 1992) and show our early result of large $I_{Cl(PLM)}$ in oocytes with no $I_{Cl(endo)}$. The triangles are from 44 oocytes studied later with large $I_{Cl(endo)}$. We now consider the possibility that PLM is not itself an ion channel, but rather modulates $I_{Cl(endo)}$.

We begin by inspecting currents in two oocytes from the same batch, one of which was injected with PLM mRNA (Fig. 6, *A* and *B*). There are some strong similarities. Both are hyperpolarization-activated, inward anion currents which do not inactivate. They share the halide selectivity sequence $I^- > NO_3^- > Br^- > Cl^-$. Neither requires Ca^{2+} , and both are blocked by Ba^{2+} in the sub-millimolar range.

There are, however, major differences. $I_{Cl(PLM)}$ is an order of magnitude larger, has a different pharmacologic profile, and its amplitude is modulated by pH. The activation kinetics are different—where $I_{Cl(endo)}$ activates as a sum of two exponentials, $I_{Cl(PLM)}$ has a sigmoidal delay and is better described as:

$$I(t) = I_o + A(1 - \exp -t/\tau_1)^N \exp -t/\tau_2.$$

Further, were $I_{Cl(PLM)}$ a modified $I_{Cl(endo)}$, one might expect that batches of oocytes with large $I_{Cl(endo)}$ would express larger $I_{Cl(PLM)}$ after RNA injection, as there would be more substrate channels for PLM to modify. $I_{Cl(PLM)}$ would then be expected to be positively correlated with $I_{Cl(endo)}$. Fig. 6 *D* suggests that this is not the case. If $I_{Cl(PLM)}$ were larger in oocytes having large $I_{Cl(endo)}$, a line through the data points would have a positive slope. The figure, on the other hand, shows no clear correlation. These results suggest that the amplitude of $I_{Cl(PLM)}$ was independent of the amplitude of $I_{Cl(endo)}$, which is not the expected result if $I_{Cl(PLM)}$ is a modified $I_{Cl(endo)}$.

Moreover, $I_{Cl(endo)}$, $I_{Cl(PLM)}$, and an $I_{Cl(PLM)}$ mutant have different voltage-dependence of activation. Fig. 7 shows families of $I_{Cl(endo)}$, $I_{Cl(PLM)}$, and $I_{Cl(F28Y)}$. The PLM mutant F28Y has a polar hydroxyl group in the middle of the transmembrane region. These records, which are from oocytes of different batches, were chosen because they had similar magnitudes of tail current. As we have reported, $I_{Cl(F28Y)}$ has faster activation kinetics than $I_{Cl(PLM)}$ (Moorman et al., 1992). The tail currents show three traces with active current for $I_{Cl(endo)}$ and $I_{Cl(F28Y)}$, but only two for $I_{Cl(PLM)}$, suggesting that $I_{Cl(PLM)}$ activates at more negative potentials. Fig. 7 *D* shows a plot of normalized tail current amplitude as a function of the voltage of a hyperpolarizing conditioning step. The data points for $I_{Cl(endo)}$ are the same as in Fig. 3 *D*. The gating valence for $I_{Cl(PLM)}$ is 2.2 charges, and significantly exceeds the value of 1.4 for $I_{Cl(F28Y)}$ as well as the value of 1.3 for $I_{Cl(endo)}$. In addition, the threshold for activation is significantly more negative for $I_{Cl(PLM)}$ than for the others, about -80 mV for activation of 0.1 to 1% of maximum current, compared with -30 to -40 mV.

$I_{Cl(PLM)}$ and $I_{Cl(endo)}$ have similarities and differences. While the differences suggest that they are two different currents, several scenarios could explain the similarities. First, PLM might modulate the $I_{Cl(endo)}$ channel—to change the activation kinetics, threshold potential, and the voltage-sensitivity of activation, membrane-bound PLM molecules would have to modify the intrinsic gating and voltage-sensing mechanisms of the $I_{Cl(endo)}$ molecule. Specifically, the hydrophobic domain of PLM would have to modify the $I_{Cl(endo)}$ voltage sensor, as $I_{Cl(PLM)}$ has a different voltage-sensitivity than $I_{Cl(endo)}$, and this change is partially reversed by the F28Y mutation. This degree of modulation has precedent, as subunits of Na^+ and Ca^{2+} channels have dramatic effects on current amplitude and gating (Lacerda, Kim, Ruth, Perez-Reyes, Flockerzi, Hofmann, Birnbaumer, and Brown, 1991; Isom, De Jongh, Patton, Reber, Offord, Charbonneau, Walsh, Goldin, and Catterall, 1992). Second, $I_{Cl(endo)}$ might flow through oligomeric complexes of PLM-like molecules which are endogenous to

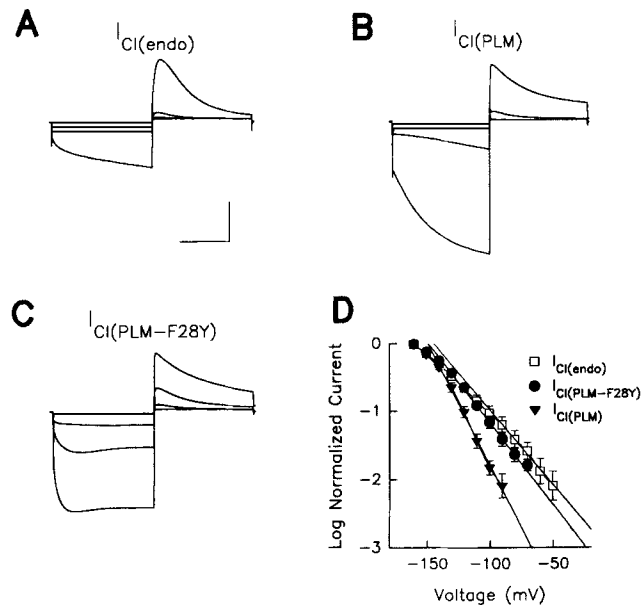


FIGURE 7. Comparison of $I_{Cl(endo)}$, $I_{Cl(PLM)}$, and $I_{Cl(F28Y)}$. Representative traces from three classes of oocytes; uninjected (A) injected with mRNA encoding (B) wildtype PLM, or (C) the PLM mutant F28Y. Hyperpolarization steps are to -30 , -90 , -120 , and -160 mV. Bar is 0.5 s and 3 μ A. The tail current for the PLM-injected oocyte is seen first after a hyperpolarization to a more negative potential than for the endogenous and mutant currents.

D shows the voltage sensitivity of activation gating. The data shown are for uninjected oocytes with large $I_{Cl(endo)}$, and for oocytes expressing wildtype PLM and the mutant F28Y; bars are standard error. Tail currents were measured at potentials of $+10$ or $+40$ mV after hyperpolarization to potentials indicated along the x-axis (-30 to -160 mV). The currents were normalized relative to the largest tail current elicited. The straight line was fit to the points from 1 to 10% of the maximum tail current. $I_{Cl(PLM)}$ showed the steepest dependence on the conditioning potential, with an estimated gating valence of 2.2 compared to 1.3 to 1.4 for $I_{Cl(endo)}$ and $I_{Cl(PLM-F28Y)}$.

Xenopus oocytes. Thus, expressed PLM molecules might incorporate into heterooligomeric complexes, forming channels with similar selectivity but different gating and drug binding properties.

Measurement of whole oocyte currents does not resolve the issue of whether PLM is an ion channel, or a modulator of $I_{Cl(endo)}$. A rigorous test of the hypothesis that PLM is itself an ion channel awaits the demonstration of anion currents through PLM molecules reconstituted in a synthetic lipid bilayer.

We thank L. Tyler Horne for his assistance. This work was supported by National Institutes of Health grants (to L. R. Jones and J. R. Moorman), the Herman C. Krannert Fund (L. R. Jones), and an American Heart Association Established Investigator Award (J. R. Moorman).

Original version received 2 June 1993 and accepted version received 12 October 1993.

REFERENCES

- Ackerman, M. J., and D. E. Clapham. 1993. Cardiac chloride channels. *Trends in Cardiovascular Medicine*. 3:23–28.
- Anderson, M. P., R. J. Gregory, S. Thompson, D. W. Souza, S. Paul, R. C. Mulligan, A. E. Smith, and M. J. Welsh. 1991. Demonstration that CFTR is a chloride channel by alteration of its anion selectivity. *Science*. 253:202–205.
- Bahinski, A., A. C. Nairn, P. Greengard, and D. C. Gadsby. 1989. Chloride conductance regulated by cyclic AMP-dependent protein kinase in cardiac myocytes. *Nature*. 340:718–721.
- Barish, M. E. 1983. A transient calcium-dependent chloride current in the immature *Xenopus* oocyte. *Journal of Physiology*. 342:309–325.
- Bear, C. E., F. Duguay, A. L. Naismith, N. Kartner, J. W. Hanrahan, and J. R. Riordan. 1991. Cl⁻ channel activity in *Xenopus* oocytes expressing the cystic fibrosis gene. *The Journal of Biological Chemistry*. 266:19142–19145.
- Blatz, A. L., and K. L. Magleby. 1983. Single voltage-dependent chloride-selective channels of large conductance in cultured rat muscle. *Biophysical Journal*. 43:237–241.
- Chesnoy-Marchais, D. 1982. A Cl⁻ conductance activated by hyperpolarization in *Aplysia* neurons. *Nature*. 299:359–361.
- Chesnoy-Marchais, D. 1983. Characterization of a chloride conductance activated by hyperpolarization in *Aplysia* neurons. *Journal of Physiology*. 342:277–308.
- Coulombe, A., H. Ducholier, E. Coraboeuf, and N. Touzet. 1987. Single chloride-permeable channels of large conductance in cultured cardiac cells of new-born rats. *European Biophysical Journal*. 14:155–162.
- Coulombe, A., and E. Coraboeuf. 1992. Large-conductance chloride channels of new-born rat cardiac myocytes are activated by hypotonic media. *Pflügers Archiv*. 422:143–150.
- Durieux, M. E., M. N. Salafranca, K. R. Lynch, and J. R. Moorman. 1992. Lysophosphatidic acid induces a pertussis toxin-sensitive Ca²⁺-activated Cl⁻ current in *Xenopus laevis* oocytes. *American Journal of Physiology*. 263:C896–C900.
- Ehara, T., and K. Ishihara. 1990. Anion channels activated by adrenaline in cardiac myocytes. *Nature*. 347:284–286.
- Franciolini, F., and W. Nonner. 1987. Anion and cation permeability of a chloride channel in rat hippocampal neurons. *Journal of General Physiology*. 90:453–478.
- Gabriel, S. E., L. L. Clarke, R. C. Boucher, and M. J. Stutts. 1993. CFTR and outwardly rectifying chloride channels are distinct proteins with a regulatory relationship. *Nature*. 363:263–268.
- Gründer, S., A. Thiemann, M. Pusch, and T. J. Jentsch. 1992. Regions involved in the opening of ClC-2 chloride channel by voltage and cell volume. *Nature*. 360:759–762.
- Harvey, R. D., and J. R. Hume. 1989. Autonomic regulation of a chloride current in heart. *Science*. 244:983–985.
- Hille, B. 1992. Ionic channels of excitable membranes. Sinauer Associates Inc., Sunderland, MA. 544 pp.
- Isom, L. L., K. S. De Jongh, D. E. Patton, B. F. X. Reber, J. Offord, H. Charbonneau, K. Walsh, A. L. Goldin, and W. A. Catterall. 1992. Primary structure and functional expression of the $\beta 1$ subunit of the rat brain sodium channel. *Science*. 256:839–842.
- Jentsch, T. J., K. Steinmeyer, and G. Schwarz. 1990. Primary structure of *Torpedo marmorata* chloride channel isolated by expression cloning in *Xenopus* oocytes. *Nature*. 348:510–514.
- Kokubun, S., A. Saigusa, and T. Tamura. 1991. Blockade of Cl channels by organic and inorganic blockers in vascular smooth muscle cells. *Pflügers Archiv*. 418:204–213.

- Lacerda, A. E., H. Kim, P. Ruth, E. Perez-Reyes, V. Flockerzi, F. Hofmann, L. Birnbaumer, and A. M. Brown. 1991. Normalization of current kinetics by interaction between the α_1 and β subunits of the skeletal muscle dihydropyridine-sensitive Ca^{2+} channel. *Nature*. 352:527–530.
- Levesque, P. C., P. J. Hart, J. R. Hume, J. L. Kenyon, and B. Horowitz. 1992. Expression of cystic fibrosis transmembrane regulator Cl^- channels in heart. *Circulation Research*. 71:1002–1007.
- Loo, D. D. F., J. G. McLarnon, and P. C. Vaughan. 1981. Some observations on the behavior of chloride current-voltage relations in *Xenopus* muscle membrane in acid solutions. *Canadian Journal of Physiological Pharmacology*. 59:7–13.
- Matsuoka, S., T. Ehara, and A. Noma. 1990. Chloride-sensitive nature of the adrenaline-induced current in guinea-pig cardiac myocytes. *Journal of Physiology*. 425:579–598.
- Miledi, R. 1982. A calcium-dependent transient outward current in *Xenopus laevis* oocytes. *Proceedings of the Royal Society of London*. 215:491–497.
- Moorman, J. R., C. J. Palmer, J. E. John, M. E. Durieux, and L. R. Jones. 1992. Phospholemman expression induces a hyperpolarization-activated chloride current in *Xenopus* oocytes. *The Journal of Biological Chemistry*. 267:14551–14554.
- Palmer, C. J., B. T. Scott, and L. R. Jones. 1991. Purification and complete sequence determination of the major plasma membrane substrate for cAMP-dependent protein kinase and protein kinase C in myocardium. *The Journal of Biological Chemistry*. 266:11126–11130.
- Parker, I., C. B. Gundersen, and R. Miledi. 1985. A transient inward current elicited by hyperpolarization during serotonin activation in *Xenopus* oocytes. *Proceedings of the Royal Society of London*. 223:279–292.
- Parker, I., and R. Miledi. 1988. A calcium-independent chloride current activated by hyperpolarization in *Xenopus* oocytes. *Proceedings of the Royal Society of London*. 233:191–199.
- Peres, A., and G. Bernardini. 1983. A hyperpolarization-activated chloride current in *Xenopus laevis* oocytes under voltage-clamp. *Pflügers Archiv*. 399:157–159.
- Rich, D. P., R. J. Gregory, M. P. Anderson, P. Manavalan, A. E. Smith, and M. J. Welsh. 1991. Effect of deleting the R domain on CFTR-generated chloride channels. *Science*. 253:205–207.
- Saigusa, A., and S. Kokubun. 1988. Protein kinase C may regulate resting anion conductance in vascular smooth muscle cells. *Biochemical and Biophysical Research Communication*. 155:882–889.
- Schwarze, W., and H. A. Kobl. 1984. Voltage-dependent kinetics of an anionic channel of large unit conductance in macrophages and myotube membranes. *Pflügers Archiv*. 402:281–291.
- Soejima, M., and S. Kokubun. 1988. Single anion-selective channel and its ion selectivity in the vascular smooth muscle cell. *Pflügers Archiv*. 411:304–311.
- Steinmeyer, K., C. Ortland, and T. J. Jentsch. 1991. Primary structure and functional expression of a developmentally regulated skeletal muscle chloride channel. *Nature*. 354:301–304.
- Taglietti, V., F. Tanzi, R. Romero, and L. Simoncini. 1984. Maturation involves suppression of voltage-gated currents in the frog oocyte. *Journal of Cellular Physiology*. 121:576–588.
- Thiemann, A., S. Gründer, M. Pusch, and T. J. Jentsch. 1992. A chloride channel widely expressed in epithelial and non-epithelial cells. *Nature*. 356:57–60.
- Vaughan, P. 1991. Substitute anions and the chloride conductance of frog muscle: effects of chlorate and bromate on steady-state values and kinetics. *Pflügers Archiv*. 419:152–159.
- Warner, A. E. 1972. Kinetic properties of the chloride conductance of frog muscle. *Journal of Physiology*. 227:291–312.
- Woll, K. H., M. D. Leibowitz, B. Neumcke, and B. Hille. 1987. A high-conductance anion channel in adult amphibian skeletal muscle. *Pflügers Archiv*. 410:632–640.